JOURNAL OF CATALYSIS **175,** 152–160 (1998)
ARTICLE NO. CA981985

Direct Partial Oxidation of Methane to Synthesis Gas by Cerium Oxide

Kiyoshi Otsuka,[1] Ye Wang, Eiyuh Sunada, and Ichiro Yamanaka

Department of Chemical Engineering, Tokyo Institute of Technology, Ookayama, Meguro-ku, Tokyo 152, Japan

Received May 16, 1997; revised November 20, 1997; accepted November 21, 1997

The gas–solid reaction between methane and cerium oxide (CeO_2) directly produced a synthesis gas with H_2/CO ratio of 2. The addition of Pt black remarkably accelerated the formation rates of H_2 and CO and decreased the activation energy for the production of the synthesis gas. The hydrogen-exchange reaction between CH_4 and CD_4 proceeded remarkably faster than the oxidation of methane with CeO_2 regardless of the presence or absence of Pt. Thus, It was suggested that the cleavage of the C−H bond of methane could not be the rate-determining step. The small kinetic isotopic effect ($k_H/k_D = 1.1 \pm 0.1$) in methane conversion suggested that the step involving hydrogen such as the recombination or desorption of hydrogen could be the rate-determining step. H_2, CO, and a small amount of CH_4 were observed in temperature-programmed desorption experiments for the chemisorbed species generated on CeO_2 during the reaction with methane. This result along with the *in situ* FT-IR spectroscopic results suggested that the reaction proceeded not through HCHO but probably through carbon intermediate. CO must be produced by the reaction of the carbon with the lattice oxygen of CeO_2. TPD experiments showed that the presence of Pt remarkably decreased the temperature for the desorptions of H_2 and CO. The obvious tailing of H_2 formation in the reaction of CeO_2 with methane pulse also indicated that the recombination or desorption of hydrogen was the rate-determining step. It was suggested that Pt accelerated this step probably through a reverse spillover mechanism.

INTRODUCTION

The chemical utilization of natural gas, one of the world's abundant resources, to produce basic chemicals is one of the desirable goals in the current chemical industry. However, because of the chemical inertness of methane, the main constituent of natural gas, the chemical transformation of natural gas directly into useful chemicals as industrial starting materials is a great challenge. The conversion of methane to useful chemicals has attracted much attention in recent years and many methods and technologies have been reported. Although the direct conversion of methane to valuable chemicals such as methanol or ethylene is the most fascinating route, no viable process or catalyst has been developed (1–3). At present, the indirect transformation of methane via synthesis gas is still the most competitive process (4). Generally, methane is converted to synthesis gas via steam reforming (5). The synthesis gas then serves as a feedstock of many chemical processes, e.g., Fischer–Tropsch and methanol syntheses. However, as shown in Eq. [1],

$$CH_4 + H_2O \rightarrow CO + 3H_2, \quad \Delta H = +49.3 \text{ kcal/mol}, \quad [1]$$

because the steam reforming is a highly endothermic reaction, the reaction has to be operated at high temperature (>900°C) and a large amount of energy is consumed to drive this reaction. Furthermore, for Fischer–Tropsch or methanol synthesis,

$$nCO + 2nH_2 \rightarrow C_nH_{2n} + nH_2O, \quad [2]$$

$$CO + 2H_2 \rightarrow CH_3OH, \quad [3]$$

the desired H_2/CO ratio is 2, thus the H_2/CO ratio of synthesis gas obtained from steam reforming must be adjusted through the reverse shift reaction. By contrast, the partial oxidation of methane to synthesis gas

$$CH_4 + \tfrac{1}{2}O_2 \rightarrow CO + 2H_2, \quad \Delta H = -8.5 \text{ kcal/mol}, \quad [4]$$

is an exothermic reaction and gives a H_2/CO ratio of 2. This reaction may proceed at much moderate temperatures (e.g., <500°C). However, the direct oxidation of methane to synthesis gas is very difficult to achieve (6, 7). Actually, most of the reports concerning the partial oxidation method involved the complete oxidation of methane to CO_2 and H_2O followed by the reforming of the remaining CH_4 with H_2O and CO_2 (8–15). As a result, a high temperature (>800°C) is required to obtain high selectivities of H_2 and CO due to the limitation of thermodynamic equilibrium of the reforming reaction at low temperatures. Although several catalysts are active in this partial oxidation of methane, a rapid deactivation of catalysts seems to be a big problem.

Recently, we tested a novel method for the direct conversion of CH_4 to synthesis gas by gas–solid reactions (16).

[1] To whom correspondence should be addressed. Telephone: (+81-3) 5734-2143; Fax: (+81-3)5734-2879; E-mail: kotsuka@o.cc.titech.ac.jp.

0021-9517/98 $25.00

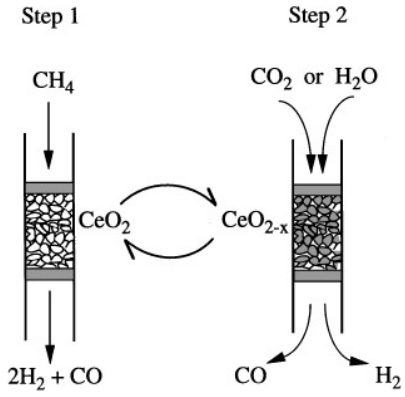

FIG. 1. Method for direct conversion of CH_4 to synthesis gas using redox of CeO_2.

This method is schematically represented in Fig. 1. CH_4 reacts with CeO_2 in step 1, producing H_2 and CO with a ratio of 2. The gas product can directly be used for the Fischer–Tropsch or the methanol synthesis. The reduced cerium oxide (CeO_{2-x}) can be recovered to CeO_2 by the reaction with CO_2 or H_2O in step 2, producing pure CO or H_2 simultaneously. Both CO and H_2 are industrially necessary chemicals for the carbonylation and hydrogenation processes, respectively. Equations [5]–[7] summarize the reactions occurring in both steps.

step 1

$$CeO_2 + xCH_4 \rightarrow CeO_{2-x} + xCO + 2xH_2 \qquad [5]$$

step 2

$$CeO_{2-x} + xCO_2 \rightarrow CeO_2 + xCO \qquad [6]$$

$$CeO_{2-x} + xH_2O \rightarrow CeO_2 + xH_2 \qquad [7]$$

The thermodynamic considerations of the reactions in Eqs. [5]–[7] are shown in Fig. 2. The oxidation of CH_4 by CeO_2 is thermodynamically viable at >600°C, while the reaction in step 2 is favorable at <700°C. Thus the two-step method described above can overcome the thermodynamic limitation at ca. 600°C. In previous papers (16), we have demonstrated that H_2 and CO with a ratio of 2 are selectively produced by the reaction of CH_4 with CeO_2 at ≥700°C. The reduced CeO_{2-x} was recovered to CeO_2 by H_2O with high efficiency in step 2, producing H_2 at 400–600°C. Compared to the reaction in step 2, the reaction in step 1, i.e., the reaction between CH_4 and CeO_2, needed considerably higher temperatures than 600°C because of lower reaction rate. Therefore, in order to increase the efficiency of this two-step method, the reaction in step 1 needs to be accelerated. The main purpose of this work is to find a suitable catalyst for the acceleration of the rate of reaction of CH_4 with CeO_2 and to clarify its catalytic function. The reaction mechanism for the formation of H_2 and CO from CH_4 is also discussed on the bases of kinetic, FT-IR, TPD, and pulse studies.

EXPERIMENTAL

Materials

The CeO_2 (purity >99.9%) purchased from Wako Chemical Industry Co. was used for the reaction. The BET surface area determined by N_2 adsorption was 6.3 m^2/g. Many metals and oxides used as catalysts or additives were thoroughly mixed with CeO_2 using an agate mortar for 1 h. The samples with the amount of the additives of 8 mol% in metal element basis for oxide additives and of 1 wt% for metal black additives were selected as representatives in this paper, because 5 and 25 mol% for the former and 0.5 wt% for the latter showed similar enhancing or retarding effects as their essential features of the effects.

Reactions

The gas–solid reaction between CH_4 and CeO_2 was carried out using a conventional fixed bed quartz reactor operated at atmospheric pressure. The inner diameter of the reactor was 8 mm. For a standard reaction, 3.0 g of CeO_2 or of the mixture of CeO_2 and catalyst was loaded in the reactor. The granules with sizes of 20–40 mesh were used. The length of the CeO_2 bed (both with and without catalyst) was ca. 4 cm. The reactor was set in an electric furnace ca. 40 cm long and a thermal homogeneous zone of

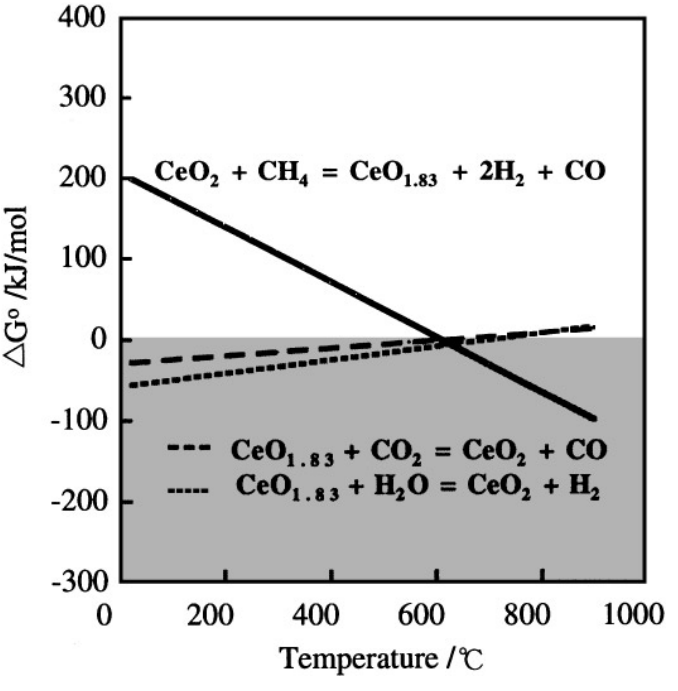

FIG. 2. Thermodynamic calculations for the reactions in steps 1 and 2. The calculation was based on the data in Ref. (20).

ca. 8 cm. The CeO_2 with or without catalyst was pretreated in an O_2 flow diluted with Ar ($P(O_2) = 50.5$ kPa, total flow rate = 120 cm^3/min) at 700°C for 1 h before the reaction. After the reactor was purged with pure Ar (99.99%, flow rate = 120 cm^3/min) for 1 h, the reaction was started by passing a CH_4 flow diluted with Ar ($P(CH_4) = 50.5$ kPa, total flow rate = 120 cm^3/min). The products were analyzed by a TCD equipped on-line gas chromatograph with an interval of ca. 10 min. An active carbon column (3 m) was used for the analysis of H_2, CO, and CH_4. H_2O and CO_2 were simultaneously analyzed by a Gaschropak-54 (3 m) column. The line between the exit of the reactor and gas chromatograph was heated to 110°C to prevent the condensation of H_2O. Because CeO_2 is the only oxygen source, the degree of reduction of CeO_2 by CH_4 could be evaluated from the total amount of the oxygen-containing products, i.e., CO, CO_2, and H_2O, as follows:

$$\text{degree of reduction} = \frac{[\text{CO}] + 2[\text{CO}_2] + [\text{H}_2\text{O}]\ (\text{mol})}{2[\text{CeO}_2]\ (\text{mol})} \times 100\ (\%).$$

The recovery of the reduced cerium oxide (step 2) after the reaction with CH_4 (step 1) was performed by reaction with CO_2 or H_2O. CO_2 or H_2O gas diluted with Ar (CO_2/Ar = 1/7 or H_2O/Ar = 1/40) at a flow rate of 40 cm^3/min was introduced to react with CeO_{2-x} after the reactor was purged with Ar. The recovery of the lattice oxygen of cerium oxide was calculated on the basis of the amount of CO or H_2 produced as follows:

$$\text{degree of recovery} = \frac{\text{amount of CO or H}_2\text{ produced in step 2}}{\text{amount of oxygen removed from CeO}_2\text{ in step 1}} \times 100\ (\%).$$

FT-IR Measurement

For IR-transmission measurement, CeO_2 or Pt-added CeO_2 was pressed into a self-supporting water. The quartz-made IR cell equipped with two NaCl windows was connected to a closed gas-circulation system linked to a vacuum line. The sample in the cell could be heated to 1000 K. The IR experiments were carried out with a Fourier-transform infrared spectrometer (JASCO FT/IR-7000) equipped with an MCT detector cooled with liquid nitrogen. All the spectra were recorded after the sample was cooled down to room temperature with a cooling water pipeline surrounding the IR cell.

Temperature-Programmed Desorption (TPD) Measurement

TPD measurements of the chemisorbed species were performed for CeO_2 and Pt-added CeO_2 after the contact with CH_4 at 650°C. After the samples being cooled down to room temperature, the gas phase was removed by evacuation to 10^{-6} Torr. TPD measurement was then carried out by increasing the temperature at a rate of 4°C/min. The desorbed products were monitored by a quadrupole mass spectrometer.

CH_4–CD_4 Exchange Reaction and Isotope Effect (k_H/k_D) Measurement

The isotope exchange reaction between CH_4 and CD_4 and the measurement of the isotope effect (k_H/k_D) on the basis of their rates of conversion were carried out using a closed gas-circulation system made of Pyrex glass. The CeO_2 or Pt-added CeO_2 powder was placed in a U-shaped quartz reactor (i.d. 4 mm) which was inserted in an electric furnace. The gases were circulated by a circulation pump during the reaction. The system was connected through a leak valve to a quadrupole mass spectrometer and to a gas chromatograph for the analysis of the products from methane.

Pulse Reaction

The same apparatus for the flow reaction described above was used for pulse reactions. For the pulse reactions, a CH_4 pulse carried with Ar was introduced to the fixed bed reactor loaded with CeO_2. The exit pulse including products were directly passed through an active carbon column, and the responses of the CH_4 and the products were recorded by an on-line gas chromatograph.

RESULTS

Gas–Solid Reaction between CH_4 and CeO_2

Figure 3 represents typical kinetic curves of the products in the reaction of CH_4 with CeO_2 at 700°C. H_2 and CO were the overwhelming products, although H_2O and CO_2 were observed at the very early stage of the reaction. The ratio of H_2 and CO was almost kept at 2.0 after 20 min of reaction. As described earlier, such a syngas with H_2/CO ratio of 2 could directly be used for the Fischer–Tropsch or the methanol synthesis.

The formation of H_2 and CO under the conditions of Fig. 3 lasted for ca. 400 min. The calculation showed that the degree of reduction of CeO_2 was 21% after the reaction, comparable to the value (25%) by assuming that CeO_2 is completely reduced to Ce_2O_3. Such an amount of oxygen consumed obviously cannot be ascribed to the surface oxygen only, because the amount of oxygen at the first surface layer on the basis of BET surface area (6.3 m^2 g^{-1}) corresponds to roughly 5% of the consumed oxygen in step 1. Therefore, it is clear that the bulk lattice oxygen of CeO_2 must participate in the oxidation of CH_4.

It should be noted in Fig. 3 that the formation of H_2 and CO continued in the absence of H_2O and CO_2 in the gas phase after 30 min. The presence of gaseous H_2O and CO_2

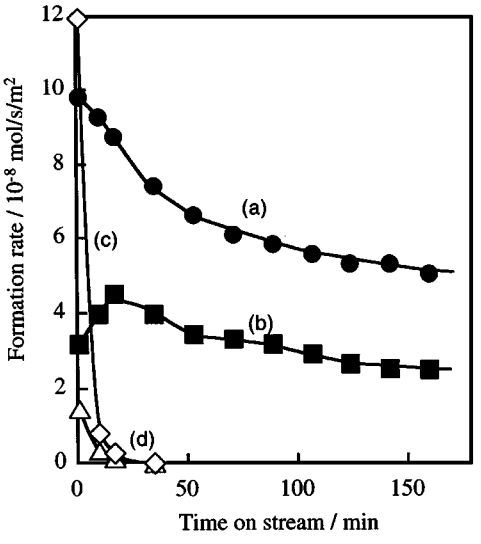

FIG. 3. Kinetic curves for the reaction of CH_4 with CeO_2: (a) H_2; (b) CO; (c) H_2O; (d) CO_2. Reaction conditions: $T = 700°C$, $P(CH_4) = P(Ar) = 50.5$ kPa, total flow rate = 120 mL/min, $CeO_2 = 3.0$ g.

at the early stage of the reaction did not particularly accelerate the formation of H_2 and CO. In order to understand the scheme for the formation of H_2 and CO, the reforming reactions of CH_4 with CO_2 were carried out on CeO_2. The reforming reaction of CH_4 with CO_2 (initial $P(CH_4) = 50$ kPa, $P(CO_2) = 5$ kPa, and $CeO_2 = 1.0$ g) always produced H_2O, and the H_2/CO ratio never did exceed 1.0 at temperatures of 600–800°C. The reforming reaction of CH_4 with H_2O was always accompanied by the formation of CO_2 and never gave the H_2/CO ratio of 2. Therefore, we believe that the H_2 and CO in Fig. 3 were not the reforming products but rather that the products formed directly from the reaction of CH_4 and CeO_2.

Carbon deposition during the reaction is an important aspect in carrying out the reaction smoothly. Thus, we measured the total amount of carbonaceous species deposited on cerium oxide after the reaction with CH_4. After the reaction, the reactor was purged with Ar, and then a pure O_2 flow (120 cm^3/min) was introduced to burn out the carbon deposited on cerium oxide. The CO and CO_2 produced were quantified by gas chromatograph and were used to calculate the amount carbon deposit. Such measurements were done by stopping the reaction of CH_4 with CeO_2 at different reaction times and thus at different degrees of CeO_2 reduction. As indicated in the previous paper (16), almost no carbon deposit was observed at a degree of reduction lower than 10%. However, the carbon deposit increased sharply when the degree of reduction was increased above 10%. Therefore, we have already claimed that it is better to keep the degree of reduction below 10% to avoid the carbon deposit in step 1 and to guarantee the repeated use of the cerium oxide in steps 1 and 2.

Oxidation of CeO_{2-x} with CO_2 and H_2O

The reduced cerium oxide (CeO_{2-x}) after the experiment in Fig. 3 (the degree of reduction was 8%) was purged with Ar and subjected to the reaction with CO_2 or H_2O. Figure 4 shows the formation rates of CO and H_2 during the reactions with CO_2 and H_2O at 450 and 550°C, respectively. Both reactions proceeded smoothly at such temperatures and finished after 20 and 40 min, respectively. The calculations showed that the degrees of recovery of CeO_2 reached 82 and 90%, respectively.

Catalyst for the Reaction between CH_4 and CeO_2

The results described above suggest that the reaction in step 2 proceeds smoothly and fast as compared with the reaction in step 1. In order to increase the efficiency of this two-step method, the reaction in step 1, i.e., the reaction between CH_4 and CeO_2, should be accelerated. Thus, many additives were tested for the oxidation of CH_4 with CeO_2. The formation rates of H_2 and CO (average rates in the initial 20 min) in the presence of different additives are shown in Fig. 5. It is known that the addition of alkaline earth metal oxides such as CaO and SrO results in the formation of solid solutions with CeO_2, generating lattice oxygen

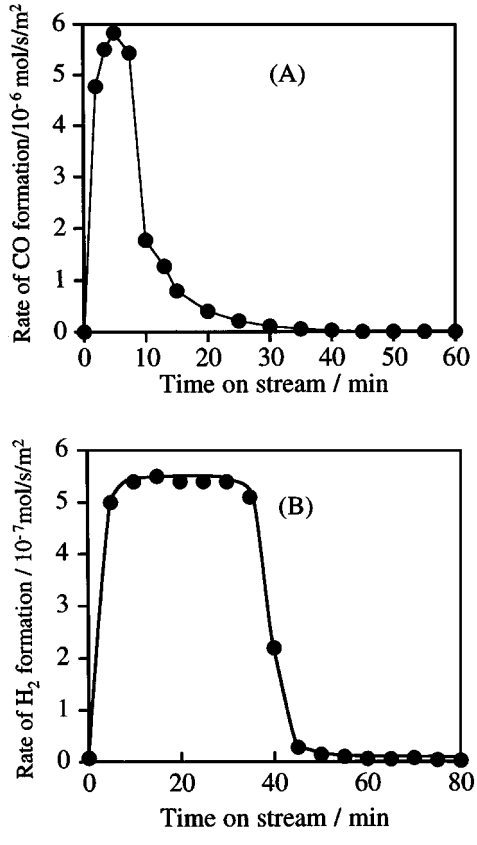

FIG. 4. Production of CO and H_2 during the reactions of the reduced cerium oxide with CO_2 (A) and H_2O (B).

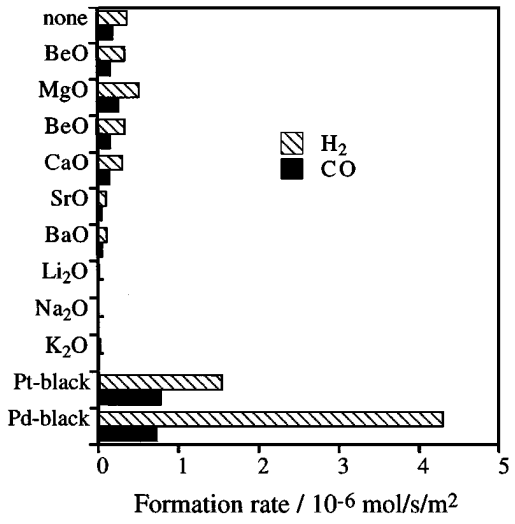

FIG. 5. Effect of additives on the formation rate of H_2 and CO.

defects (17). The diffusion of lattice oxygen anion could thus be accelerated. However, the formation rates of both H_2 and CO were not appreciably enhanced by the addition of these alkaline earth metal oxides as shown in Fig. 5. Therefore, the diffusion of lattice oxygen might not be a rate-determining step in the reaction of CH_4 with CeO_2. The addition of alkali metal oxides, i.e., Li_2O, Na_2O, and K_2O remarkably decreased the formation rates of H_2 and CO. On the other hand, the presence of Pt black or Pd black obviously accelerated the formation of H_2 and CO. Figure 5 shows that the formation rate of H_2 is highest in the presence of Pd black. However, the H_2/CO ratio obtained was ca. 6.0, which notably exceeded the stoichiometric ratio of H_2/CO (= 2.0) expected in Eq. [5]. This high H_2/CO ratio indicates the deposit of carbon on Pd-added CeO_2. On the other hand, in the case of Pt, the ratio of H_2/CO was 2.05. Thus, Pt accelerated the stoichiometric reaction of Eq. [5] without depositing carbon.

The reaction of CH_4 with Pt black (30 mg) without CeO_2 produced only a small amount of H_2 (ca. 1% of that in the presence of CeO_2). The formation of CO was not observed at all. Therefore, Pt functioned as a catalyst for the reaction of CH_4 with CeO_2.

The formation rates of CO at different reaction temperatures for both CeO_2 and Pt-added CeO_2 were measured previously (16). The formation rate of CO was increased in the presence of Pt at all the temperatures investigated. It should be noted that the ratio of H_2/CO was always 2.0 ± 0.1 irrespective of the reaction temperature. The apparent activation energy for the formation of CO was decreased from 160 to 68 kJ/mol due to the presence of Pt. This result strongly supports the idea that Pt black has a very notable catalytic function on the formation of CO and H_2.

The degrees of reduction of CeO_2 after the reaction with CH_4 for 2 h at different temperatures were plotted in Fig. 6. Pt black enhanced the degrees of reduction of CeO_2 at all the reaction temperatures, and such enhancement became more notable at lower temperatures. The oxidation of CH_4 with CeO_2 became notable at ca. 550°C in the presence of Pt catalyst, while temperatures ≥650°C were required when the catalyst was absent.

In Situ FT-IR Measurement

As described above, it was demonstrated that H_2 and CO with a ratio of 2 could be selectively produced from the gas–solid reaction of CH_4 with CeO_2, and this reaction was accelerated by Pt catalyst. The elucidation of the mechanism for the formation of H_2 and CO is important in understanding the role of Pt. One possibility is that H_2 and CO may be formed through intermediates such as absorbed CH_3O or HCHO. Thus, *in situ* FT-IR measurements have been carried out to investigate the adsorbed species. Figure 7 shows the spectra obtained after the reaction of CH_4 (5.3 kPa) with Pt-added CeO_2 (wafer with a diameter of 3 cm and a weight of 80 mg) in IR cell at 550°C for 2 h. The spectra were recorded within 10 min after the sample was quenched to room temperature. Difference spectra are shown here, in which the absorbance arising from the Pt–CeO_2 sample itself is subtracted. No obvious absorption peak is observed in the region of OH and C–H stretching vibrations (3500–2500 cm^{-1}), except for the stretching of C–H ascribed to gaseous CH_4 (sharp peak at 3016 cm^{-1}). This indicates that the species comprising C–H and O–H due to the adsorbed HCHO and CH_3OH or due to their precursors or derivates may not be formed on the surface of Pt–CeO_2 during the reaction. Furthermore, the absorption bands ascribed to the stretching of C=O in HCHO, which should appear at 1650–1800 cm^{-1}, were not observed as shown in Fig. 7B.

On the other hand, four absorption peaks at 1576, 1296, 1030, and 860 cm^{-1} were observed, and these peaks could

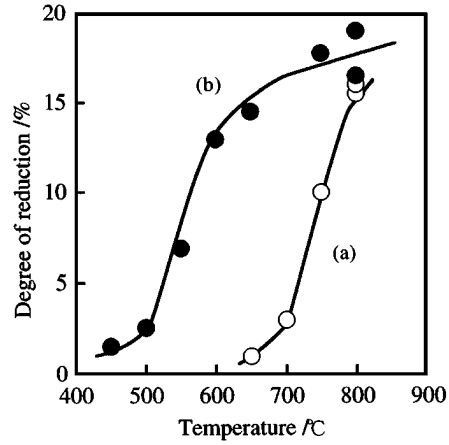

FIG. 6. Dependence of the reduction degree of CeO_2 on the reaction temperature: (a) CeO_2; (b) Pt–CeO_2. Reaction conditions: $P(CH_4) = P(Ar) = 50.5$ kPa; total flow rate = 120 mL/min; $CeO_2 = 3.0$ g.

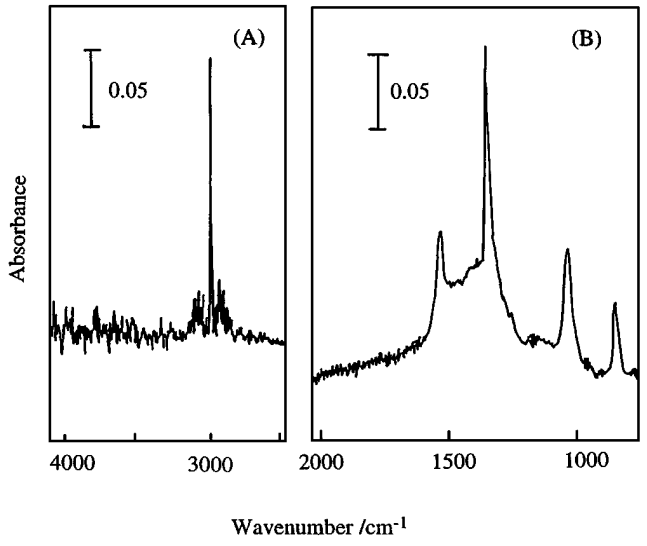

FIG. 7. FT-IR spectra recorded after the reaction of CH_4 with Pt-added CeO_2.

be ascribed to a bidentate-type carbonate with a structure as below (18).

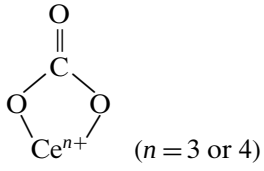

$(n = 3 \text{ or } 4)$

It is very usual that carbonate species exists on the surface of cerium oxide because of the basicity of cerium oxide. However, whether there is a correlation between the carbonate species and the formation of CO is unclear at this moment.

As a conclusion of IR measurements, the absorption bands which could be assigned to CH_x, methoxide (CH_3O), and HCHO species were not observed. Although we cannot exclude the situation that the lifetime of these species is too short or the steady-state concentration of these species is too low to be detected by FT-IR spectroscopy, this result more likely indicates that the reaction does not proceed through these intermediates.

TPD Measurement

To obtain further information about the possible reaction intermediates and to understand the effect of Pt on the formation of the products, the desorption features of the chemisorbed species on CeO_2 with and without Pt were investigated by TPD method. The experiments were carried out in the following sequences. Before TPD measurements, the reaction of CeO_2 with CH_4 in the presence and absence of Pt had been performed at 650°C for 1 h, the reactor was then cooled down to room temperature within 10 min. The TPD measurements for the chemisorbed species on CeO_2 with and without Pt were then carried out after the gas phase in the reactor had been removed by evacuation to ca. 10^{-6} Torr. The heating rate used for TPD measurement was 4°C/min. The products desorbed were monitored by a mass spectrometer.

The result for CeO_2 was shown in Fig. 8A, only the desorptions of H_2 and CO along with a trace of CH_4 were observed. The desorptions of both H_2 and CO occurred almost simultaneously and started at ca. 250°C. The fact that HCHO was not observed in this experiment supports the speculation that the reaction does not proceed through a HCHO intermediate.

The TPD results in the presence of Pt black are shown in Fig. 8B. In this case, the main desorption products were also H_2 and CO. However, the commencement temperature for the desorption of both H_2 and CO was obviously lowered due to the presence of Pt black. It should be noted that no CO was observed and only a very small amount of H_2 (<1% of the total H_2 desorbed in Fig. 8B) was desorbed when only Pt was used. Thus, Pt lowered the temperature for the desorption of H_2 and CO which had been adsorbed on cerium oxide. Besides H_2 and CO, the desorption of CH_4 was also observed and its amount was increased in the presence of Pt. The adsorption of CH_4 on CeO_2 was studied in detail by Li and Xin using FT-IR spectroscopy (19). They reported

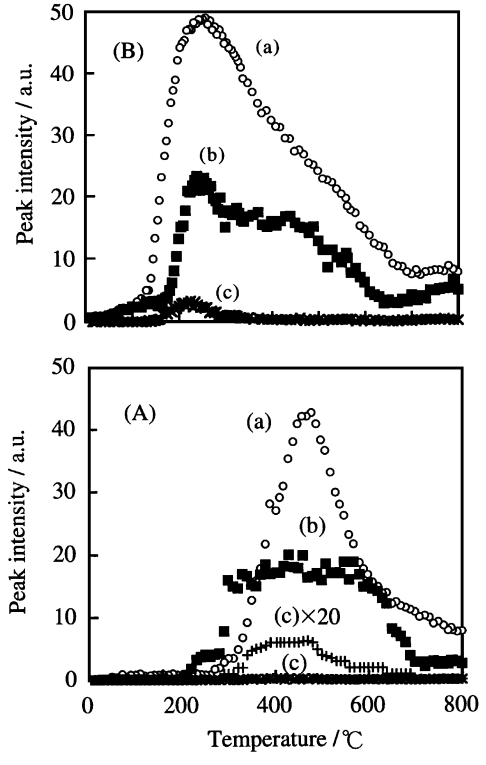

FIG. 8. TPD curves after the reaction of CH_4 with CeO_2 (A) and Pt–CeO_2 (B): (a) H_2; (b) CO; (c) CH_4.

that CH_4 could only be adsorbed on CeO_2 at temperatures lower than −15°C. Thus, it is unlikely that the CH_4 desorbed at 150–300°C in Fig. 8 results from the adsorbed CH_4 itself on CeO_2. Moreover, since the peak temperature for the desorption of CH_4 was very close to those of H_2 and CO, we speculate that this CH_4 arises through the hydrogenation of adsorbed carbon species, a probable reaction intermediate. Thus, it is likely that the adsorbed carbon and hydrogen atoms may serve as the intermediates for the formation of H_2 and CO.

CH_4–CD_4 Exchange Reaction

Hydrogen exchange reaction between CH_4 and CD_4 was carried out to obtain information about the dissociation of C–H bond of CH_4. Figure 9 shows the result of the CH_4–CD_4 exchange reaction on CeO_2 at 650°C. The reaction was carried out using a closed gas-circulation system. The initial CH_4/CD_4 ratio was 12/13. Both CH_4 and CD_4 concentrations decreased steeply with reaction time at early stage of the reaction (<10 min). Simultaneously, the hydrogen-exchanged products, i.e., CH_3D, CHD_3, and CH_2D_2, were formed and their concentrations increased along the reaction time. However, their concentrations did not change appreciably after 20 min.

A quantitative calculation showed that at least 149 μmol of methane molecules exchanged their hydrogen and deuterium during CH_4–CD_4 reaction in the first 10 min on CeO_2 without Pt. However, the amount of methane converted to CO was only 2 μmol under such reaction conditions. This result means that the CH_4–CD_4 exchange reaction proceeds much more rapidly than the oxidation of methane on CeO_2. This is also true of the case in the presence of Pt. Thus, the cleavage of C–H bond of methane could not be the rate-determining step in the overall oxidation of CH_4 with CeO_2.

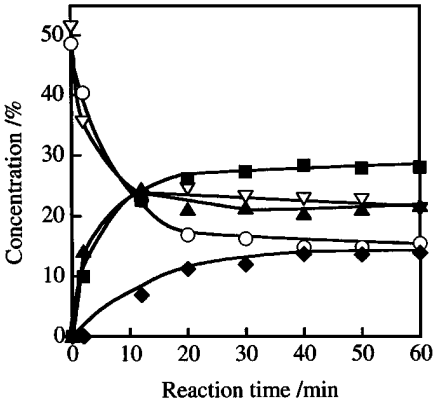

FIG. 9. Results for the hydrogen exchange between CH_4 and CD_4 over CeO_2: (○) CH_4; (▽) CD_4; (■) CH_3D; (▲) CHD_3; (◆) CH_2D_2. Reaction conditions: $CeO_2 = 3.0$ g, $T = 650$°C, $P(CH_4) = P(CD_4) = 2.7$ kPa.

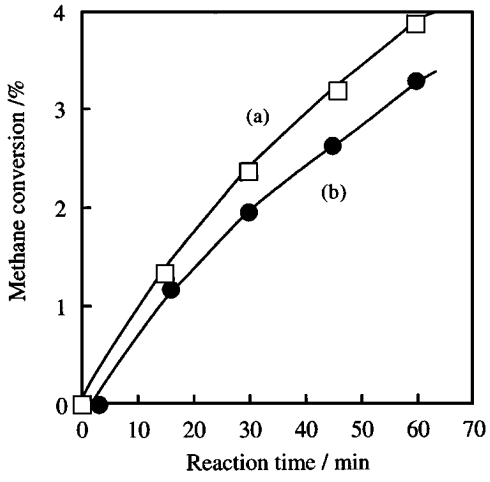

FIG. 10. Conversion of CH_4 and CD_4 versus reaction time: (a) CH_4; (b) CD_4. Reaction conditions: $CeO_2 = 3.0$ g, $T = 650$°C, $P(CH_4) = P(CD_4) = 2.7$ kPa.

Isotope Effect in the Oxidation of Methane

In order to get further knowledge about the rate-determining step in the overall reaction of methane with CeO_2, the isotope effect (k_H/k_D) was measured by comparing the conversion rates of CH_4 and CD_4. The reactions of CH_4 and CD_4 with CeO_2 were performed using a closed gas-circulation system under the same conditions. The conversions of CH_4 and CD_4 versus reaction time are shown in Fig. 10.

Similar to the results obtained in the reactions using the gas flow system described earlier, the products for these experiments were also mainly CO and H_2 or D_2. The slopes of the curves at the initial stage of the reaction (<30 min) in Fig. 10 showed that the isotope effect (k_H/k_D) for the conversion of methane was 1.1 ± 0.1. This low isotope effect may not contradict the suggestion obtained from the CH_4–CD_4 exchange reaction, i.e., the cleavage of the C–H bond is not the rate-determining step in the overall reaction of methane into H_2 and CO. We consider that this low isotope effect is caused by other elementary steps involving hydrogen, probably the formation of H_2 through the recombination of H atoms or the desorption of H_2.

Pulse Reaction

The reaction of CeO_2 with CH_4 pulses was carried out to get further information about the mechanism for the reaction between CeO_2 and CH_4 and the formation of H_2 and CO. The transient responses of the product pulses were shown in Fig. 11. For the first CH_4 pulse, the formation of CO_2 was observed. The formation of CO_2 may be a result of the reaction of CH_4 with the active oxygen on CeO_2 surface. However, no CO was observed for the first to third CH_4 pulse reactions. The formation of CO was observed

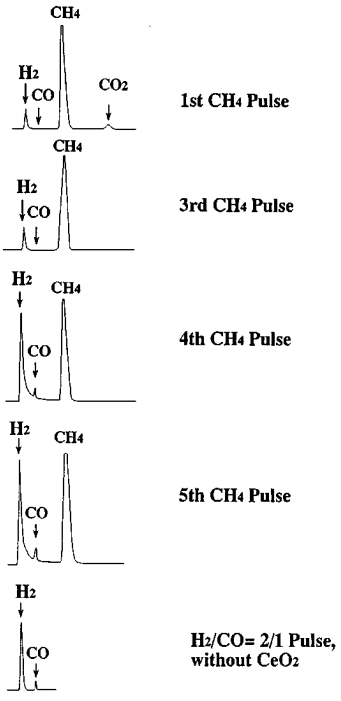

FIG. 11. Transient responses for the reaction of CeO_2 with CH_4 pulse. Reaction conditions: $CeO_2 = 3.0$ g, $T = 700°C$, CH_4 pulse size 50 μL.

from the fourth pulse of CH_4 and the H_2 peak was sharply increased simultaneously. It should be noted that the sensitivity of the TCD detector was 10 times higher for H_2 than for CO_2 or CO. Thus, the observed H_2 peak was much larger than that of CO. The experimental results mentioned above imply that the reduced sites on CeO_2, i.e., the sites with Ce^{3+} and oxygen anion vacancies which are generated in the reactions of first to third CH_4 pulses, may be important for the selective formation of H_2 and CO.

Another experimental fact which should be noted is the remarkable tailing of the H_2 peak observed from the fourth CH_4 pulse. However, such notable tailing was not observed for CH_4 and CO peaks. Moreover, no tailing of H_2 peak was observed when a H_2/CO pulse with a ratio of 2/1 was injected to the reactor in the absence of CeO_2 (the last response peaks in Fig. 11). These observations imply that the desorption of H_2 from a slightly reduced cerium oxide is a slow step. Thus we speculate that the recombination of H atoms or the desorption of H_2 could be the rate-determining step in the formation of synthesis gas.

DISCUSSION

As described above, we have reported a novel method for the selective conversion of CH_4 to H_2 and CO with a ratio of 2 by gas–solid reaction between CH_4 and CeO_2 in the absence of gaseous O_2. Here, it should be stressed again that CeO_2 acts as not a catalyst but an oxidant for the oxidation of CH_4. The formation rate of H_2 and CO can be remarkably enhanced by adding Pt as a catalyst. The CeO_{2-x} after the reaction with CH_4 (step 1) can be recovered by reactions with CO_2 and H_2O (step 2), producing pure CO and H_2, respectively. The separation of the two steps is important, since the catalytic reaction of CH_4 with CO_2 or H_2O on CeO_2 did not give H_2 and CO with a ratio of 2 without producing H_2O or CO_2.

The FT-IR experiments suggested that the formation of H_2 and CO would not proceed through intermediates such as adsorbed CH_3OH (or CH_3O) and HCHO. The TPD measurement for the chemisorbed species after the reaction of CH_4 with CeO_2 suggested that adsorbed carbonaceous species and hydrogen atoms were probably the reaction intermediates. Thus, we speculate that the reaction may proceed as follows:

$$CH_4 \rightarrow C(a) + 4H(a), \qquad [8]$$

$$4H(a) \rightarrow 2H_2, \qquad [9]$$

$$xC(a) + CeO_2 \rightarrow xCO + CeO_{2-x}. \qquad [10]$$

A further detailed reaction mechanism which we have in mind is shown in Fig. 12. As suggested by the results of the pulse reaction experiments (Fig. 11), the reduced surface sites, i.e., Ce^{3+} and oxygen vacancy, must be responsible for the activation of CH_4 for the selective production

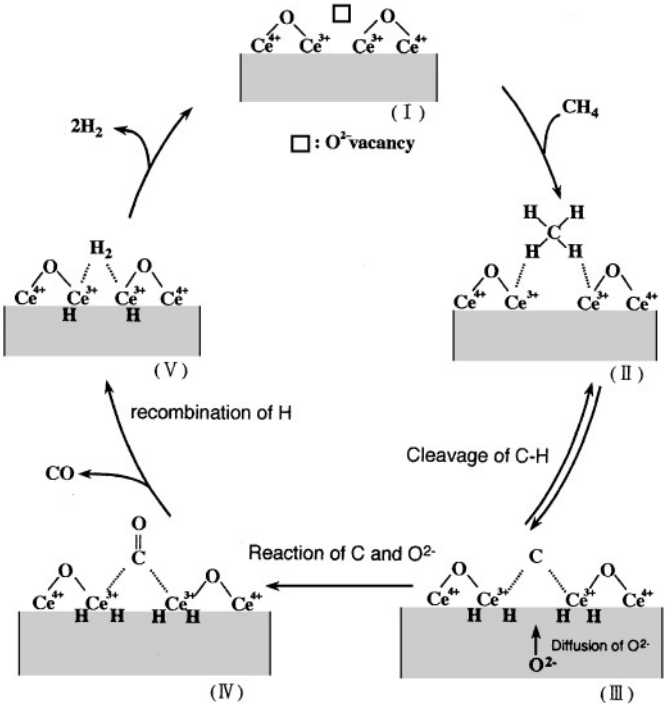

FIG. 12. Reaction mechanism for the formation of H_2 and CO from the reaction of CH_4 with CeO_2; (□) oxygen vacancy.

of H_2 and CO. The carbon and hydrogen atoms thus formed might be adsorbed in the vacancies near Ce^{3+}. The rapid CH_4–CD_4 exchange reaction and the small isotope effect ($k_H/k_D = 1.1 \pm 0.1$ at 650°C) suggested that the cleavage of CH_4 on the Ce^{3+} sites was not the rate-determining step.

CeO_2 is the only oxygen source in the oxidation of CH_4. The degree of reduction of cerium oxide after a complete reaction with CH_4 (until neither H_2 nor CO formation was observed) reached 21%, suggesting that almost all the CeO_2 was reduced to Ce_2O_3. Obviously, such a large amount oxygen consumed cannot be ascribed only to the surface oxygen of CeO_2. Thus, the lattice oxygen must be responsible for the formation of CO. The experimental fact that the improvement of the diffusion of the lattice oxygen does not increase the formation rates of H_2 and CO allows us to speculate that the diffusion of lattice oxygen is not the rate-determining step in the overall reactions.

The low isotope effect ($k_H/k_D = 1.1 \pm 0.1$) is consistent with the results of CH_4–CD_4 exchange reactions that the cleavage of CH_4 is not the rate-determining step. This low isotope effect further indicates that another elementary step involving hydrogen atoms must control the reaction. The obvious tailing of H_2 in the transient response pulse reaction suggests that the step for the formation of H_2, which involves the recombination of hydrogen atoms and the desorption of H_2, is a slow step. The presence of Pt accelerates this step as shown by the TPD measurement. We speculate that this enhancement may be achieved by a reverse spillover mechanism, viz., the spillover of H atoms trapped in the surroundings of Ce^{3+} to Pt sites where the recombination of H atoms or the desorption of H_2 must occur more facilely.

ACKNOWLEDGMENTS

Part of this work has been carried out as a research project of Japan Petroleum Institute commissioned by the Petroleum Energy Center with the subsidy of the Ministry of International Trade and Industry.

REFERENCES

1. Brown, M. J., and Parkyns, N. D., *Catal. Today* **8**, 305 (1991).
2. Krylov, O. V., *Catal. Today* **18**, 209 (1993).
3. Crabtree, R. H., *Chem. Rev.* **95**, 987 (1995).
4. Fox, J. M., III, *Catal. Rev.-Sci. Eng.* **35**, 169 (1993).
5. Van Hook, J. P., *Catal. Rev.-Sci. Eng.* **21**, 1 (1980).
6. Hickman, D. A., and Schmidt, L. D., *J. Catal.* **138**, 267 (1992).
7. Hickman, D. A., and Schmidt, L. D., *Science* **259**, 343 (1993).
8. Ashcroft, A. T., Cheetham, A. K., Foord, J. S., Green, M. L. H., Grey, C. P., Murrel, A. J., and Vernon, P. D. F., *Nature* **344**, 319 (1990).
9. Jones, R. H., Ashcroft, A. T., Waller, D., Cheetham, A. K., and Thomas, J. M., *Catal. Lett.* **8**, 169 (1991).
10. Vernon, P. D. F., Green, M. L. H., Cheetham, A. K., and Ashcroft, A. T., *Catal. Today* **13**, 417 (1992).
11. Dissanayake, D., Rosynek, M. P., Kharas, K. C. C., and Lunsford, J. H., *J. Catal.* **132**, 117 (1991).
12. Dissanayake, D., Rosynak, M. P., and Lunsford, J. H., *J. Phys. Chem.* **97**, 3644 (1993).
13. Nakamura, J., Umeda, S., Kubushiro, K., and Kunimori, K., and Uchijima, T., *J. Jpn. Pet. Inst.* **36**, 97 (1993).
14. Choudhary, V. R., Rajput, A. M., and Prabhakar, B., *J. Catal.* **139**, 326 (1993).
15. Vermeiren, W. J. M., Blomsma, E., and Jacobs, P. A., *Catal. Today* **13**, 427 (1992).
16. Otsuka, K., Ushiyama, T., and Yamanaka, I., *Chem. Lett.,* 1517 (1993); Otsuka, K., Sunada, E., Ushiyama, T., and Yamanaka, I., *Stud. Surf. Sci. Catal.* **107**, 531 (1997).
17. Etsell, T. H., and Flengas, S. N., *Chem. Rev.* **70**, 339 (1970).
18. Bozon-Verduraz, F., and Bensalem, A., *J. Chem. Soc., Faraday Trans.* **90**, 653 (1994).
19. Li, C., and Xin, Q., *J. Phys. Chem.* **96**, 7714 (1992).
20. MALT2, The Japan Society of Calorimetry and Thermodynamic Analysis, Tokyo, 1993.